

FIG. 2. (Color online) GIAS scans for different angles of incidence: (a) high, (b) intermediate, and (c) low doses. The angular positions of (111) and (220) reflections in crystalline Si are shown as vertically dotted lines. The lowest lines show the scattering signal from an untreated Si area. The dashed lines are simulated in terms of Debye model.

(1×10^{17} ions/cm²) to high (7×10^{17} ions/cm²). All samples were prepared using a high current ion implanter facility at Saha Institute, for optimized incident angle ($\sim 60^\circ$) and energy (60 keV).

The x-ray experiments were carried out at the beamline ID01 of the European Synchrotron Radiation Facility (Grenoble, France). The beamline is especially designed to achieve a large tunable energy range, good energy resolution, and a low background. The experiments were performed using a nanopatterned Si crystal with a (001) surface orientation. All measurements were carried out for x-ray energy of 8 keV. By GID technique one can investigate the structural properties associated with the crystalline part of nanostructure. The GID profiles confirmed the existence of lateral undulation (or buried ripples) at the interface between amorphous and crystalline parts of the sample only for high dose Ar⁺ bombardment of the present experiment. The wavelength and the amplitude of the buried ripples derived from the GID profiles confirmed the results of TEM observation.^{10,11} The wavelength (about 700 nm) and amplitude (about 60 nm) of the top-surface ripples were estimated with the AFM which was consistent with the previous study.¹³ The ripple wave vector in the present experiment was parallel to the projection of ion beam on the surface and also to the [1-10] direction. In order to understand the amorphous peculiarities of the surface ripples we applied a GIAS method. Here we choose the in-plane incidence angle θ to a position outside any Bragg condition at a fixed incident angle α_i . A position-sensitive detector was moved in plane in a large range of 2θ angle from 8° to 60° .

Figure 2 shows GIAS profiles for the three samples under investigation. The scattering pattern from implanted area is dominated by two broad maxima on top of an amorphous background. For comparison we have also measured the

GIAS from the nonirradiated Si that shows a monotone decreasing behavior. The dashed line in Fig. 2(a) is a simulated GIAS profile for a highly damaged structure obtained under the high dose of irradiation. This profile was simulated based on Debye formula¹⁴ for the intensity of x-ray scattering of more than 300 next neighbor distances where both the nearest neighbor distance ($d_1=2.35$ Å) and a next-neighbor distance ($d_2=3.84$ Å) for Si are modified. The curve clearly demonstrates that the maximum positions of the humps correspond to the (111) and (220) lattice planes of crystalline state and broadening of the width reflects the high disorder of next neighbor distances as it is typical for an amorphous solid.¹⁵ Exactly such behavior takes place for the high dose of irradiation with GIAS peak positions (2θ) at 28.5° and 47.3° , as shown in Fig. 2(a). The intensity of both broad peaks decreases as a function of dose. Additionally, the GIAS peaks are shifted to smaller 2θ angles [Figs. 2(b) and 2(c)] and the level of the amorphous background is decreased. The positions of the first and second peaks for the intermediate and low dose samples move to 25° , 24° and 45° , 44° , respectively. This can be explained by a lattice expansion due to a high concentration of defects. The dashed lines in Figs. 2(b) and 2(c) are simulations by Debye's formula under similar constraints as mentioned above with $d_1=2.6$ Å, $d_2=4.2$ Å and $d_1=2.7$ Å, $d_2=4.4$ Å, correspondingly. The same change of nearest neighbor distances was found by tight-binding simulations of structural features at the crystalline-amorphous Si interface.¹⁶

The transition layer between the amorphous surface ripples and the crystalline buried rippled interface contains highly damaged crystalline and completely amorphous regions. As shown in Fig. 2 the GIAS intensity saturates at a certain incident angle corresponding to certain information depth. One can estimate this transition layer thickness of about 10 nm for lowest dose (saturation at $\alpha_i=0.1^\circ$) but about 50–60 nm for highest dose (saturation at $\alpha_i=0.2^\circ$), demonstrating that the transition layer thickness increases with irradiation dose. Supplementary to the amorphous scattering a few samples show narrow peaks [see Fig. 2(a) and 2(c)] representing highly strained small crystallites. Their intensities become large at shallow α_i confirming the surface arrangement of these crystalline clusters. They may be formed during wafer preparation/manipulation process before irradiation, because such peaks were found on the nonirradiated area as well. In contrast to nonirradiated Si the irradiation causes strain and therefore shifts of the 2θ positions and the appearance of fcc-forbidden reflections such as (100), (200), and (112).

In order to understand the directional anisotropy of GIAS coming from the implanted region we have performed GIAS scans at various azimuth angles (ω) of the sample. Figure 3(a) shows such a map for the low dose sample under investigation. Strong intensity lines appear at different ω on the background of a complete amorphous scattering signal. The map can be interpreted by a texture of the defect-rich regions of the transition layer. The GIAS map of the high dose sample looks to be similar in appearance [see Fig. 3(b)]. It also shows a texture of defect-rich regions on top of a much higher amorphous background.

The obtained results strongly support the assumption that the buried crystalline ripple formation in Si depends on the direction of irradiation with respect to crystallographic lattice of the sample. As was mentioned before, a well pro-

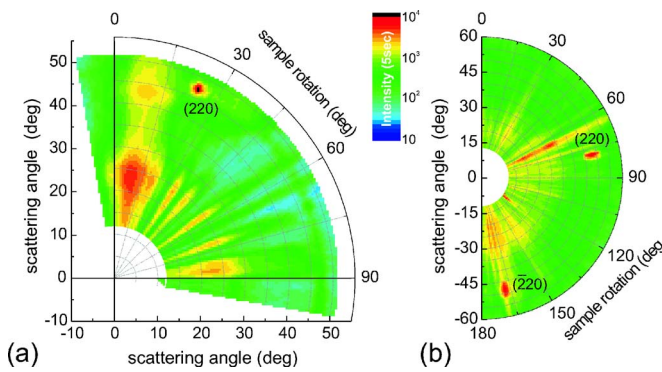


FIG. 3. (Color online) 2θ - ω amorphous maps of the sample after low dose (a) and after highest dose of implantation (b) at an incidence angle of 0.05° .

nounced formation of ripples could be achieved only if the incident angle of ion beam is directed towards the $[1-10]$ azimuth direction and is close to 60° with respect to the surface normal. For Si(001) surfaces the ion beam strongly interacts with (110) atomic planes making an angle of 54.7° between $[111]$ and $[001]$. This angle is very close to the irradiation angle, which is known with an accuracy of few degrees only due to experimental reasons. If the energy of the ion beam is high enough many Si chains will be broken along the beam path. The damage might be different in the direction perpendicular to the ion beam, i.e., for (1-10) atomic planes. Along this direction the interaction of implanted ions with host atoms is less intense because most of the momentum transfer is directed towards $[1-10]$. Therefore one can assume that the (1-10) crystal planes remain less damaged in the case of the low dose of irradiation. However, due to the defects created along (1-10) the (110) lattice spacing might differ from that of the perfect crystal. This affects the (111) and (110) atomic planes and interplanar distances that become firstly deformed during implantation. The shift of the GIAS peaks to the smaller 2θ values suggests an increase of nearest and next nearest neighbor distances due to inclusions of defects (interstitials). Moreover, as shown in Figs. 2 and 3, the transition layer is not completely amorphous and shows strong azimuthal anisotropy of the highly defect-rich crystalline units. These textured crystalline units are created during the ion irradiation and are separated from each other by amorphous regions. This is consistent with the knowledge that an Ar^+ irradiation with energies exceeding 20 keV can produce several amorphous zones in individual subcascades, most of which are spatially well separated^{17,18}

At low ion doses the crystallites might be large and strained due to the incorporation of a large number of defects. With increasing ion dose the size of the textured crystallite decreases accompanied by a strain release due to the increase of amorphous regions in their neighborhood. Our model is supported by TEM inspection as well. Both low-

damaged and highest-damaged samples show a transition layer with nonuniform contrast but increasing number of misoriented crystallites close to the interface to crystalline bulk region.

In summary, our findings suggest a scenario for dose-dependent damage at medium energies of Ar^+ implantation of silicon: a highly damaged layer is created below the rippled surface. It consists of two parts, a textured crystalline and a complete amorphous part. The ratio of both parts changes with dose. These new findings of microstructural anisotropy caused by nonuniform interaction along different particular crystallographic directions may have an important role in the formation of buried crystalline ripples for keV argon bombarded silicon surface. Moreover, we have seen so far that the top-surface ripple is conformal to the buried crystalline ripple structure and as a result improvement in the model descriptions is required to understand the ion-beam-induced ripple-structure formation process.

The authors would like to thank H. Metzger for the support at the beamline ID01 at ESRF. This work was supported by the DST-DAAD India-Germany Collaborative Program.

- ¹C. Hofer, S. Abermann, C. Teichert, T. Bobek, H. Kurz, K. Lyutovich, and E. Kasper, Nucl. Instrum. Methods Phys. Res. B **216**, 178 (2004).
- ²A. Toma, F. B. de Mongeot, R. Buzio, G. Fipro, S. R. Bhattacharyya, C. Boragno, and U. Valbusa, Nucl. Instrum. Methods Phys. Res. B **230**, 551 (2005).
- ³U. Valbusa, C. Boragno, and F. B. de Mongeot, J. Phys.: Condens. Matter **14**, 8153 (2002).
- ⁴R. M. Bradley and J. M. E. Harper, J. Vac. Sci. Technol. A **6**, 2390 (1988).
- ⁵M. A. Makeev, R. Cuerno, and A.-L. Barabasi, Nucl. Instrum. Methods Phys. Res. B **197**, 185 (2002).
- ⁶T. K. Chini, M. K. Sanyal, and S. R. Bhattacharyya, Phys. Rev. B **66**, 153404 (2002).
- ⁷S. Facsko, T. Bobek, A. Stahl, H. Kurz, and T. Dekorsy, Phys. Rev. B **69**, 153412 (2004).
- ⁸M. Castro, R. Cuerno, L. Vazquez, and R. Gago, Phys. Rev. Lett. **94**, 016102 (2005).
- ⁹R. Gago, L. Vaazquez, R. Cuerno, M. Varela, C. Ballesteros, and J. M. Albella, Appl. Phys. Lett. **78**, 3316 (2001).
- ¹⁰T. K. Chini, F. Okuyama, M. Tanemura, and K. Nordlund, Phys. Rev. B **67**, 205403 (2003).
- ¹¹S. Hazra, T. K. Chini, M. K. Sanyal, J. Grenzer, and U. Pietsch, Phys. Rev. B **70**, 121307(R) (2004).
- ¹²V. Holy, U. Pietsch, and T. Baumbach, *High Resolution X-ray Scattering from Thin Films and Multilayers*, Springer Tracts in Modern Physics, Vol. 149 (Springer, Berlin, 1999), p. 264.
- ¹³D. P. Datta and T. K. Chini, Phys. Rev. B **71**, 235308 (2005).
- ¹⁴B. E. Warren, *X-ray Diffraction* (Addison-Wesley/Dover, New York, 1990), p. 381.
- ¹⁵R. Zallen, *The Physics of Amorphous Solids* (Wiley, New York, 1983), p. 251.
- ¹⁶N. Bernstein, M. J. Aziz, and E. Kaxiras, Phys. Rev. B **58**, 4579 (1998).
- ¹⁷M. J. Caturla, T. D. Rubia, L. A. Margus, and G. H. Gilmer, Phys. Rev. B **54**, 16683 (1996).
- ¹⁸K. Nordlund, M. Ghaly, R. S. Averback, M. Caturla, T. D. Rubia, and J. Tarus, Phys. Rev. B **57**, 7556 (1998).